

# The Spin-Wave Resonance Study of Concentrational Inhomogeneities in Nanocrystalline Ni–Fe–P and Ni–Fe–C Alloys

R. S. Iskhakov, D. E. Prokof'ev, L. A. Chekanova, and V. S. Zhigalov

Kirenskiĭ Institute of Physics, Siberian Division, Russian Academy of Sciences, Krasnoyarsk, Russia

Received December 4, 2000

**Abstract**—The films of nanocrystalline Fe–Ni alloys obtained by various methods in the permalloy composition range (~20 at. % Fe) were studied by the method of spin-wave resonance (SWR) spectroscopy. The effective SW exchange stiffness  $\eta^{\text{eff}}$  exhibits a characteristic dependence on the spin wavelength, which is indicative of the magnetization fluctuations in these films with a correlation radius of 12–20 nm. This is indirect evidence of the microphase separation in these nanocrystalline alloys and provides an estimate of the characteristic spatial size of an inhomogeneity in the atomic ratio  $X_{\text{Fe}}/X_{\text{Ni}}$ . © 2001 MAIK “Nauka/Interperiodica”.

**Introduction.** As is known, nanocrystalline (NC) materials are essentially thermodynamically nonequilibrium systems characterized by a high level of internal stresses, a large concentration of defects, developed grain boundaries, and some other factors accounting for the increased thermodynamic potential  $\Delta G$  [1, 2]. This leads to the formation of metastable phases in NC alloys [3, 4] and makes these alloys capable of structural transformations that are impossible in thermodynamically equilibrium states. These unusual processes include the dissociation of hydrides [5], the decomposition of thermodynamically stable intermetallic compounds [6], etc.

Another example of such structural transformations is offered by the microphase separation (concentrational inhomogeneity), which we observed in Ni–Fe alloys with compositions in the permalloy concentration range (~20 at. %). In the single- or polycrystalline state, these alloys are classified as disordered ideal (or regular) solid solutions with an fcc crystal lattice the sites of which are randomly occupied by Fe and Ni atoms. Previously, it was believed that the statistical fluctuations of the relative atomic content  $X_{\text{Fe}}/X_{\text{Ni}}$  are small, with the fluctuation volume not exceeding more than 1 nm, which corresponds to the atomic and phase (chemical) homogeneity limits. However, our experiments showed that the nanocrystalline state stimulates a chemical inhomogeneity in these alloys, with the spatial scale exceeding 10 nm for fluctuations in the atomic ratio  $X_{\text{Fe}}/X_{\text{Ni}}$ .

Evidence for this concentrational inhomogeneity was obtained by spin-wave resonance (SWR). The idea was that a chemical or phase inhomogeneity in alloys based on the 3d transition metals (Fe, Co, Ni) is unavoidably manifested by fluctuations of the spin system parameters (exchange parameter  $\alpha$ , magnetiza-

tion  $M$ , magnitude and orientation of the local anisotropic magnetic field). These fluctuations can be detected by structurally sensitive magnetic methods such as SWR.

**Sample preparation and experimental methods.** The SWR spectra of thin-film samples of Ni–Fe–P and Ni–Fe–C alloys were measured at room temperature on a standard X-band spectrometer with a cavity pumping frequency of  $f = 9.2$  GHz using standing spin waves with wavevectors in the range from  $10^5$  to  $2 \times 10^6$  cm<sup>-1</sup>. The film samples were placed into a region of the maximum amplitude of the ac magnetic field in the duplex cavity and magnetized perpendicularly to the film surface. In this geometry, the resonance field strengths corresponding to peaks in the SWR spectrum are known to obey the equation

$$H_n = \frac{\omega}{\gamma} + 4\pi M - \alpha M k_n^2, \quad (1)$$

where  $\omega$  is the frequency,  $\gamma$  is the gyromagnetic ratio,  $\alpha$  is the exchange parameter (related to the exchange interaction constant  $A$ ),  $M$  is the magnetization, and  $k_n$  is the wavevector of the  $n$ th SWR mode. The last quantity is determined by the formula  $k_n = \pi n/d$ , where  $n = 1, 2, 3, \dots$ , and  $d$  is the film thickness.

The resonance field strengths determined in the SWR spectra were plotted in the coordinates  $\delta H = H_1 - H_n$  versus  $n^2$  (Fig 1), which allowed the experimental data to be compared to a theoretical dispersion curve  $\omega(k^2)$  calculated for the spin waves. The  $\omega(k^2)$  curve for an inhomogeneous ferromagnet was calculated in [7, 8], where it was demonstrated that the dispersion law is described by the equation

$$\omega(k) = \omega_0 + \alpha g M k^2 (1 - \gamma_i^2 J_i(k)). \quad (2)$$

Here,  $\omega_0/g$  is the internal field in the ferromagnet;  $i = \alpha$  or  $M$  (fluctuating parameter);  $\gamma_i = \Delta i/i$  is the intensity of the fluctuating parameter  $i$ ; and  $J_i(k)$  is a function set by fluctuations of the spin parameter ( $\alpha$ ,  $M$ ). The shape of the function  $J_i(k)$  determines the SW dispersion law corresponding to the fluctuations of a given spin parameter. In our case, it is important that the functions  $J_\alpha(k)$  and  $J_M(k)$  depend on the wavevector  $k$  in a significantly different manner in the region of  $k_i^* = 1/r_i^*$  determined by the correlation radius  $r_i^*$ . Indeed, the values of  $J_\alpha(k)$  in the vicinity of  $k = k^*$  increase (from 1/3 to 5/4), whereas  $J_M(k)$  first decreases from 1/2 to 0 and then (for  $k = 2k^*$ ) increases from 0 to 5/4. Because of this difference in behavior of the  $J_\alpha(k)$  and  $J_M(k)$  functions at  $k \sim k^*$ , the experimentally determined values of the effective SW stiffness  $\eta^{\text{eff}}(k)$  calculated by the formula

$$\eta^{\text{eff}}(k) = \left(\frac{d}{\pi}\right)^2 \frac{(H_1 - H_n)}{(n^2 - 1)} \quad (3)$$

will also differ provided that the wavevector interval studied contains the  $k^*$  value. In the case of the SW exchange fluctuations, the  $\eta^{\text{eff}}$  values decrease in the vicinity of  $k = k^*$ ; for the magnetization fluctuations, the  $\eta^{\text{eff}}$  values increase at  $k = k^*$  and decrease at  $k = 2k^*$ . Such changes in the behavior of  $\eta^{\text{eff}}(k)$  were previously detected by SWR in the films of amorphous ferromagnetic alloys [9–12].

The NC films of Ni–Fe–P alloys with various compositions ( $X_{\text{Ni}} = 91\text{--}71$  at. %;  $X_{\text{P}} = 2$  at. %) and thicknesses within  $\sim 150\text{--}200$  nm were obtained by chemical vapor deposition (CVD) onto glass substrates [10]. The relative content of iron and nickel ( $X_{\text{Fe}}/X_{\text{Ni}}$ ) was determined by X-ray emission spectroscopy, and the phosphorus concentration was determined by chemical analysis.

Using the X-ray diffraction techniques, the NC film samples were characterized by the symmetry (fcc), lattice constant ( $a = 3.52\text{--}3.54$  Å), and the coherent scattering domain (CSD) size (20–26 nm). The effective magnetization determined by the ferromagnetic resonance (FMR) method was  $M^{\text{eff}} = 530\text{--}660$  G; the exchange interaction constant determined from the SWR data was  $A^{\text{eff}} = (0.4\text{--}0.7) \times 10^{-6}$  erg/cm. Note that the Ni–P (iron-free) NC alloy films exhibited an FMR spectrum with a very broad band. As the alloy was doped with iron, the band width gradually decreased and then (in films with  $X_{\text{Fe}} = 8$  at. %) the spectrum showed an SWR signal containing up to 11 peaks (Fig. 2, I). An analysis of the SWR spectra showed that NC films of the Ni–Fe–P alloy system are described by the boundary conditions close to the ideal Kittel conditions (infinite pinning of the surface spins). As can be seen from Fig. 2 (I), intensities of the odd SWR peaks significantly (by more than two orders of magnitude) exceed those of the neighboring even peaks.

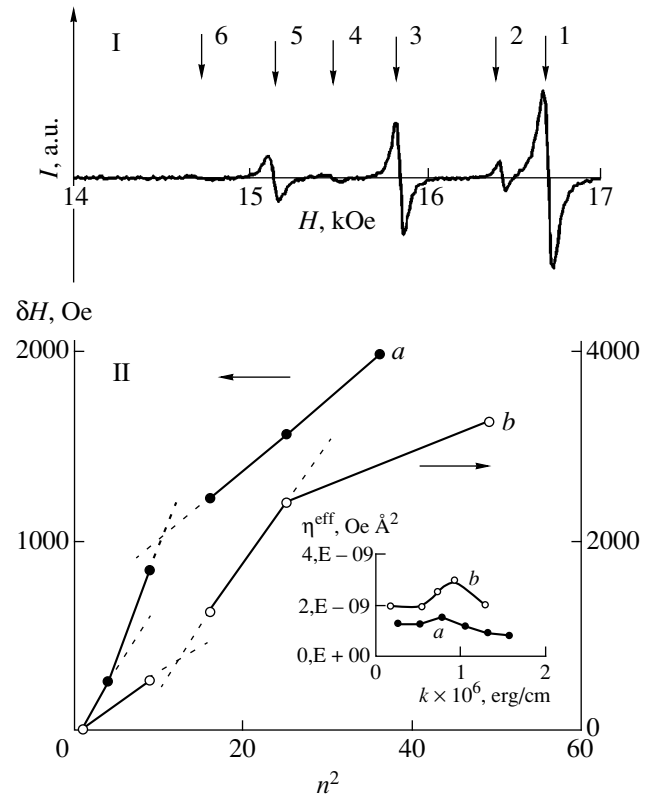


**Fig. 1.** SWR data for nanocrystalline Ni–Fe–C alloys: (I) a typical SWR spectrum of a film with the thickness  $d = 120$  nm; (II) Experimental plots of the resonance field difference  $\delta H$  versus square mode number  $n^2$  for the samples of (a)  $(\text{Ni}_{65}\text{Fe}_{35})\text{-C}$ ,  $d = 120$  nm and (b)  $(\text{Ni}_{80}\text{Fe}_{20})\text{-C}$ ,  $d = 170$  nm. The inset shows the plots of effective exchange stiffness  $\eta^{\text{eff}}$  versus wavevector for the same films.

The NC films of the Ni–Fe–C system with the compositions  $(\text{Ni}_{80}\text{Fe}_{20})\text{-C}$  and  $(\text{Ni}_{65}\text{Fe}_{35})\text{-C}$  ( $X_{\text{C}} = 15$  at. %) and thicknesses  $\sim 120\text{--}170$  nm were prepared by pulsed plasma deposition (PPD) in a vacuum [13] at a residual pressure of  $P_0 = 5 \times 10^{-6}$  Torr. The PPD samples (as well as the CVD ones) were deposited onto glass substrates. The chemical composition of these films was determined using the Auger electron spectra measured on a Riber photoelectron spectrometer (these measurements were performed at the Institute of Semiconductor Physics, Siberian Division, Russian Academy of Sciences, Novosibirsk). Also determined in these measurements were the depth–concentration profiles of the films, showing the constant content of each element. However, the phase composition exhibited variation with depth [14], for which reason these films were characterized only by the FMR spectra.

In order to measure the SWR spectrum as well, the NC films of the Ni–Fe–C system were annealed for 1 h at  $T_0 = 150, 350,$  and  $500^\circ\text{C}$  under ultrahigh vacuum conditions. This treatment resulted in the transformation of the  $(\text{Ni}_{80}\text{Fe}_{20})\text{-C}$  and  $(\text{Ni}_{65}\text{Fe}_{35})\text{-C}$  supersaturated solid solutions (CSD size,  $\sim 4$  nm) into ordered

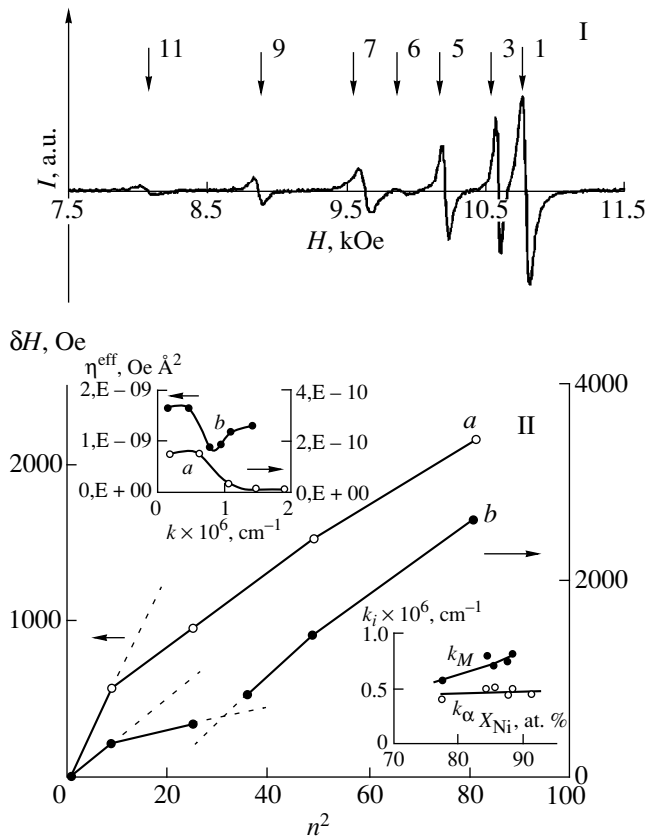


**Fig. 2.** SWR data for nanocrystalline Ni–Fe–P alloys: (I) a typical SWR spectrum of a film with the thickness  $d = 200$  nm; (II) Experimental plots of the resonance field difference  $\delta H$  versus square mode number  $n^2$  for the samples of (a)  $(\text{Ni}_{0.91}\text{Fe}_{0.09})_{98}\text{P}_2$ ,  $d = 150$  nm and (b)  $(\text{Ni}_{0.88}\text{Fe}_{0.12})_{98}\text{P}_2$ ,  $d = 190$  nm. The top inset shows the plots of effective exchange stiffness  $\eta^{\text{eff}}$  versus wavevector for the same films. The bottom inset shows the plots of wavevectors versus alloy composition for inflection points of the (open circles) “exchange”  $k_\alpha$  and (black circles) “magnetization”  $k_M$  type.

solid solutions of the hcp  $\text{Ni}_3\text{C}$  and orthorhombic  $\text{Fe}_3\text{C}$  types, respectively, followed by decomposition into  $\text{Ni}_{80}\text{Fe}_{20}$  and  $\text{Ni}_{65}\text{Fe}_{35}$  nanocrystalline alloys with an fcc lattice ( $a = 3.55\text{--}3.56$  Å), a CSD size of  $\sim 40$  nm, an exchange constant  $A \sim 0.8 \times 10^{-6}$  erg/cm, and a magnetization of  $M^{\text{eff}} = 860$  and  $1155$  G, respectively. The films of both annealed alloys exhibited SWR signals (Fig. 1, I) containing 6–7 peaks. An analysis of these spectra showed that the samples also provide for the nearly ideal (Kittel) conditions of the surface spin pinning: intensities of the odd SWR peaks significantly by more than one order of magnitude exceed those of the neighboring even peaks.

**Results and discussion.** Figure 1 (II) shows the plots of  $\delta H$  versus  $n^2$  determined from the SWR spectra of the  $(\text{Ni}_{80}\text{Fe}_{20})\text{--C}$  and  $(\text{Ni}_{65}\text{Fe}_{35})\text{--C}$  films with the thicknesses  $d = 170$  and  $120$  nm, respectively. As can be

seen, both dispersion curves of  $\delta H(n^2) \sim \omega(k^2)$  exhibit two special points (inflections) corresponding to the wavevectors  $k'$  and  $k''$ . The nanocrystalline  $\text{Ni}_{80}\text{Fe}_{20}$  alloy is characterized by  $k' = 0.52 \times 10^6$   $\text{cm}^{-1}$  and  $k'' = 0.94 \times 10^6$   $\text{cm}^{-1}$ , while the nanocrystalline  $\text{Ni}_{65}\text{Fe}_{35}$  alloy has  $k' = 0.5 \times 10^6$   $\text{cm}^{-1}$  and  $k'' = 0.93 \times 10^6$   $\text{cm}^{-1}$ . The inset in Fig. 1 (II) shows the experimental plots of  $\eta^{\text{eff}}(k)$  for the same films, which indicate that the  $\eta^{\text{eff}}$  value is increasing at  $k'$  and decreasing at  $k''$ . This behavior, as well as the characteristic shape of the experimental plot of  $\delta H(n^2) \sim \omega(k^2)$  is evidence that variation of the SW dispersion law observed in this system is determined by fluctuations of the magnetization  $M$ . This is additionally confirmed by a comparison of the  $k'$  and  $k''$  values, which is close to the theoretically predicted ratio:  $k'' = 2k'$  [7, 8].

By experimentally determining the value  $k' \approx k^*$ , we may estimate the correlation radius for the magnetization fluctuations. Using the data of Fig. 1 (II), we obtain  $r_M = 19$  nm for the films of the nanocrystalline  $\text{Ni}_{80}\text{Fe}_{20}$  alloy and  $r_M = 20$  nm for the nanocrystalline  $\text{Ni}_{65}\text{Fe}_{35}$  alloy. These spatial fluctuations of the magnetization  $M = 1/v_0 \sum_{v_0} \mu_{\text{at}}$  (see the standard definitions of  $\mu_{\text{at}}$  and the volume  $v_0$ ) can be explained only by the spatially inhomogeneous distribution of Ni and Fe atoms, whereby  $X_{\text{Fe}}/X_{\text{Ni}} = f(r)$ . Additional evidence is provided by estimates of the magnetic inhomogeneity manifested by the fluctuation intensity  $\gamma_M$  (see Eq. (2)). For the films of a nanocrystalline Fe–Ni alloy, this quantity was equal to  $\sim 0.4$ . We may use this value to estimate the possible deviations in the  $X_{\text{Fe}}/X_{\text{Ni}}$  atomic ratio from the average value, which yields variations of up to  $\sim 20$  at. %.

Figure 2 (II) shows the  $\delta H(n^2)$  plots for films of the Ni–Fe–P alloys. Here, the character of the dispersion law  $\delta H(n^2) \sim \omega(k^2)$  depends on the alloy composition. For the  $(\text{Ni}_{0.91}\text{Fe}_{0.09})_{98}\text{P}_2$  alloy (curve a), the behavior is as follows:  $\eta^{\text{eff}}(k)$  decreases at  $k = k^*$  (see the top inset in Fig. 2, II) and the  $\delta H(n^2)$  plot exhibits inflection at which the slope decreases. In terms of [7, 10], this inflection point is referred to as the “exchange type.” Determination of the  $n^*$  value corresponding to this point led to  $k_\alpha^* = 0.4 \times 10^6$   $\text{cm}^{-1}$ . For the  $(\text{Ni}_{0.88}\text{Fe}_{0.12})_{98}\text{P}_2$  alloy (curve b), there is an inflection point of the “exchange type” at  $k_\alpha^* = 0.6 \times 10^6$   $\text{cm}^{-1}$  and another inflection, at which the slope increases, while the  $\eta^{\text{eff}}(k)$  plot accordingly changes from decrease to increase.

This behavior of the dispersion curve (and the corresponding variation of  $\eta^{\text{eff}}(k)$  in the top inset in Fig. 2, II) is possible provided that the effects of  $\alpha$  and  $M$  fluctuations add to one another, which implies that the wavevector  $k' = 1.05 \times 10^6$   $\text{cm}^{-1}$  is equivalent to the  $k_M^*$  value. Note that the  $\omega(k^2)$  curve corresponding to fluc-

tuations of the magnetization  $M$  exhibits two features at  $k = k_M$  and  $2k_M$  (see Fig. 1 (II) and the previous section). In our case, the experimental dispersion curve  $\delta H(n^2)$  for the films of nanocrystalline alloys of the Ni–Fe–P system occurs at  $k < 2k_M$ . For example, an estimate of the boundary wavevector  $k$  obtained from the last peak of the SWR spectrum of a  $(\text{Ni}_{0.88}\text{Fe}_{0.12})_{98}\text{P}_2$  alloy (curve  $b$ ) is  $k_b = 1.8 \times 10^6 \text{ cm}^{-1} < 2k_M = 2.1 \times 10^6 \text{ cm}^{-1}$ .

The bottom inset in Fig. 2 (II) shows the concentration dependence of the wavevectors  $k_\alpha^*$  and  $k_M^*$  for films of the nanocrystalline Ni–Fe–P alloys. As can be seen, the  $k_M$  value linearly increases with  $X_{\text{Ni}}$ , while  $k_\alpha$  is virtually constant. Note also that the character of the  $\eta^{\text{eff}}(k)$  or  $\delta H(n^2)$  curves exhibiting inflection points of the “magnetization type” depends on the second component concentration. Estimates of the fluctuation intensity  $\gamma_i$  ( $\gamma_\alpha$ ,  $\gamma_M$ ) (see Eq. (2)) for Ni–Fe–P films of all compositions yield comparable values  $\gamma_\alpha = 0.5$  and  $\gamma_M = 0.45$ . Upon calculating the corresponding boundary wavevectors, we may estimate the spatial fluctuations of the exchange constant and the magnetization. For the alloys studied, these fluctuations are characterized by  $r_\alpha \approx 20$  and  $r_M \approx 12\text{--}17$  nm.

The films of nanocrystalline Ni–Fe–P alloys represent a ternary system of the transition metal (Ni)–transition metal (Fe)–metalloid (P) type. We believe that the fluctuations of  $\alpha$  in systems of this type are related to the inhomogeneous distribution of phosphorus in the film, whereas the fluctuations of magnetization are due to the inhomogeneous distribution of the  $X_{\text{Fe}}/X_{\text{Ni}}$  atomic ratio. In our opinion, this is confirmed by the character of variation of the  $k_\alpha$  and  $k_M$  values as functions of  $X_{\text{Fe}}/X_{\text{Ni}}$  (see the bottom inset in Fig 2, II). Thus, the SWR spectra of the films of nanocrystalline Ni–Fe alloys with compositions in the permalloy range reveal the effects caused by the microphase separation (concentration inhomogeneity) of Ni and Fe with a spatial size of these fluctuations comparable with the coherent scattering domain size.

## REFERENCES

1. A. I. Gusev, Usp. Fiz. Nauk **168** (1), 55 (1998) [Phys. Usp. **41**, 49 (1998)].
2. R. A. Andrievskii and A. M. Glezer, Fiz. Met. Metalloved. **88**, 50 (1999); **89**, 91 (2000).
3. R. S. Iskhakov, S. V. Stolyar, D. E. Prokof'ev, *et al.*, Pis'ma Zh. Éksp. Teor. Fiz. **70**, 727 (1999) [JETP Lett. **70**, 736 (1999)].
4. R. S. Iskhakov, S. V. Stolyar, L. A. Chekanova, *et al.*, Pis'ma Zh. Éksp. Teor. Fiz. **72**, 457 (2000) [JETP Lett. **72**, 316 (2000)].
5. V. A. Teplov, V. P. Pilyugin, V. S. Gaviko, *et al.*, Fiz. Met. Metalloved. **84** (5), 96 (1997).
6. C. E. Rodríguez Torres, F. N. Sánchez, and L. A. Mendoza Zeilis, Phys. Rev. B **51**, 12142 (1995).
7. V. A. Ignatchenko and R. S. Iskhakov, Zh. Éksp. Teor. Fiz. **75** (4), 1438 (1978) [Sov. Phys. JETP **48**, 726 (1978)]; R. S. Iskhakov, L. A. Chekanova, S. Ya. Kiparisov, *et al.*, Preprint No. 238F, AN SSSR, Sib. Otd., Inst. Fiz. im. L. V. Kirenskogo (Kirenskiĭ Institute of Physics, Siberian Division, USSR Academy of Sciences, Krasnoyarsk, 1984).
8. M. V. Medvedev, Fiz. Met. Metalloved. **67** (5), 876 (1989).
9. R. S. Iskhakov, M. M. Brushtunov, A. G. Narmonev, and I. A. Turpanov, Fiz. Met. Metalloved. **79** (5), 122 (1995).
10. V. A. Ignatchenko, R. S. Iskhakov, L. A. Chekanova, and N. S. Chistyakov, Zh. Éksp. Teor. Fiz. **75** (2), 653 (1978) [Sov. Phys. JETP **48**, 328 (1978)].
11. L. J. Maksimowicz and R. Zuberek, J. Magn. Magn. Mater. **58**, 303 (1986).
12. R. S. Iskhakov, M. M. Brushtunov, and A. S. Chekanov, Fiz. Tverd. Tela (Leningrad) **29** (9), 1214 (1987) [Sov. Phys. Solid State **29**, 1553 (1987)].
13. V. S. Zhigalov, G. I. Frolov, L. I. Kveglis, *et al.*, Fiz. Tverd. Tela (St. Petersburg) **40**, 2074 (1998) [Phys. Solid State **40**, 1878 (1998)].
14. A. A. Novakova, E. A. Gan'schina, T. Yu. Kiseleva, *et al.*, in *Abstracts of the Moscow International Symposium on Magnetism, Moscow, 1999*, p. 259.

*Translated by P. Pozdeev*